Muxworthy, A. R., and W. Williams (2006), Low-temperature viscous magnetization of multidomain magnetite: Evidence for disaccommodation contribution, *J. Magn. Magn. Mater.*, *307*, 113-119.

Low-temperature viscous magnetization of multidomain magnetite: evidence for disaccommodation contribution.

Adrian R. Muxworthy

School of Ocean and Earth Science, University of Southampton, European Way, Southampton, SO14 3ZH, UK.

Wyn Williams

Institute of Earth Science, University of Edinburgh, Kings Buildings, West Mains Road, Edinburgh, EH9 3JW, UK.

Co-responding author:

Adrian Muxworthy

Email: adrian.muxworthy@soton.ac.uk

Abstract

Low-temperature viscous acquisition and decay measurements above and below the Verwey transition have been measured for a selection of natural and synthetic multidomain magnetite samples. A strong correlation between the viscosity spectra and published disaccommodation spectra was found, where disaccommodation reflects electron mobility. Assuming the viscosity is controlled by identical mechanisms as disaccommodation, the reduction in electron mobility below the Verwey transition is found to significantly increase viscous acquisition and decay rates over the time scales measured (1-3000 seconds). Although strongly affecting the viscosity, disaccommodation processes do not appear to control the rate of change of viscosity with time, i.e., the viscosity curvature. It is suggested that the curvature is controlled by the shape of relaxation-time distributions, which is approximately the same for all the magnetite samples studied. In addition, the acquisition and decay curvature parameters mirror each other when plotted as a function of temperature, inferring that at any given temperature the acquisition and decay processes are identical.

PAC numbers: 75.60.Lr, 75.60.Ch, 9.60.Pn.

Keywords: magnetic viscosity, magnetic after-effect, disaccommodation, magnetite, multidomain

Introduction

On any change of a magnetic field the magnetization of a ferromagnetic system relaxes towards a new equilibrium state. If the rate of this change is of the same order of time as the problem of interest, then the magnetization is said to be viscous. The change can be due to switching of the magnetic moments in single-domain (SD) systems or the movement of domain walls in multidomain (MD) grains. The time-scale of interest may be of the order of a few pico-seconds for people examining magnetic switching mechanisms or millions of years for geologists trying to identify overprinting of an original remanence.

There are various mechanisms which are thought to contribute to the viscous behaviour in magnetic materials, but assuming no chemical alteration only two are likely to be significant for magnetite in small fields ($\leq$ 1 mT): (1) thermal fluctuations and (2) diffusion after-effects [1]. For SD assemblages of magnetite the thermal fluctuation theory of Walton [2], which extended Néel's [3] theory to include grain distributions, has been experimentally shown to accurately describe SD viscous behaviour above magnetite's Verwey transition at ~125 K, T_V [4, 5].

In contrast, MD magnetite's viscous behaviour is less well described by thermal fluctuations theories [6-8]. MD thermal fluctuation models assume that once a domain wall has reached a local energy minimum (LEM), it will remain there until a sufficiently large thermal fluctuation event occurs for it to jump into a new LEM. These LEM positions are often related to pinning sites in the crystal structure, such as dislocation lines, impurities etc. However, it is also possible for these pinning localities to move due to stress relaxation (dislocation creep), especially at high temperatures. Obviously if a pinning site moves, then a pinned domain wall will also move. The temperature dependent diffusion of dislocations is an example of a diffusion after-effect, and it is thought that MD viscosity is controlled by a combination of both thermal fluctuations and diffusion after-effects [1, 9, 10], although the relative importance of these processes is elusive. Another diffusion effect is disaccommodation, which is attributed to delayed rearrangements of defect-induced local anisotropies which arise due to

magnetocrystalline interactions with the spontaneous magnetization in domain walls [11, 12]. In the literature, the expression magnetic-after effect (MAE) is also commonly used to describe disaccommodation [11].

Disaccommodation processes and the magnetic history of the sample are interwoven since the longer a sample has been in a steady field or zero-field before a change in the field the greater the degree of diffusive re-ordering, and the smaller the viscous magnetization [13, 14]. In general the amount of disaccommodation will increase with the number of vacancies, although there are a number of mechanisms controlling disaccommodation in magnetite, and together these give rise to a complex temperature dependency [11, 15]. However it should be possible to discriminate between dislocation creep and disaccommodation since they contribute to viscosity in fundamentally different ways. Dislocation creep causes a change in the pre-existing magnetization, i.e., there is movement from one magnetic state to another. Disaccommodation, on the other hand, causes a resistance to change; it hardens the magnetic structure [16].

The behaviour of MD viscosity above room temperature displays a complex variation with its thermal history, making it difficult to truly isolate contributions from thermal activation, dislocation creep and disaccommodation effects [1, 10]. In this paper, however, we examine MD magnetite viscosity below room temperature. There are a number of differences between above and below room temperature viscosity measurements. First, thermal contributions are reduced by the lowering of the temperature. Second, dislocation creep is effectively removed since in this study the samples had been at room temperature for some considerable time (in the case of a natural single crystal several million years), reducing dislocation creep to effectively zero on the time scale of the viscosity experiments. Third, below T_V disaccommodation processes increase significantly (Fig. 1), which allows us to better assess the relationship between disaccommodation and viscosity.

On cooling below T_V, magnetite's crystallographic structure changes from cubic to monoclinic, and there is a sharp decrease in electrical conductivity due to reduced electron hopping

between Fe^{2+} and Fe^{3+} cations on B-sublattice sites [11, 17]. This decrease in electron mobility increases disaccommodation, i.e., electron mobility is reduced to the same order of time as the disaccommodation spectra measurements (~1-100 seconds). Below T_V disaccommodation is attributed to various re-ordering and tunnelling processes, and depends strongly on the stoichiometry of the magnetite, e.g., near-stoichiometric magnetite displays a strong disaccommodation peak at 300 K, which is reduced in stoichiometric magnetite [18]. In addition, below T_V there is large increase in the intensity of the magnetocrystallographic anisotropy and a change in its symmetry [19, 20]. There are also corresponding changes in many other magnetic properties [17, 21].

There have been only a limited number of studies which have investigated the viscosity of magnetite at low-temperature. Below T_V, the viscosity of SD magnetite was observed by Worm et al. [5] not to confirm to predictions of thermal fluctuation theory, but was enhanced compared to room-temperature measurements, although no physical mechanism for the enhancement was suggested. Shimizu [22] also found that the viscosity rate was also enhanced below the Verwey transition, but this time for MD magnetite, although this phenomenon was not discussed in the text. On comparison of the low-temperature disaccommodation spectra with the limited published low-temperature viscosity data, then there is reason to believe that disaccommodation will contribute significantly to the magnetic viscosity below T_V, and it is this issue that this investigation addresses.

2 Samples and Instrumentation.

The samples come from three origins; sample *W(11 μm)* was obtained from Wright Industries, was produced by crushing giving rise to relatively high levels of internal stress and irregularly shaped particles. Samples from the same material have already been described in previous studies [10]. Sample *H(23 μm)* was recently produced by hydrothermal re-crystallization [23]. Sample *E(2 mm)* was a natural single octahedral crystal of approximately 2 mm in size. It was collected from green schist on the Shetland Isles, UK. Mössbauer spectroscopy and X-ray diffraction (XRD) showed that both synthetic samples were stoichiometric or near-

stoichiometric magnetite (Table 1), whilst *E(2 mm)* was found to contain traces of hematite [24]. The bulk magnetic hysteresis properties of the three MD samples studied in this paper are summarized in Table 1. Hysteresis data, in particular the coercive force (H_C) values, suggest *W(11 μm)* has a higher concentration of dislocations and internal stress than the other two samples, which both have very low H_C values. Reflected light microscopy observations on a sister samples of *E(2 mm)* found visible impurities and inclusions not readily seen in samples *W(11 μm)* and *H(23 μm).* Warming curves for all three samples imparted with a saturation isothermal remanence (SIRM) at 5 K, display sharp Verwey transitions, in particular *H(23 μm)* (Fig. 2). Such behavior and high Verwey transition temperatures (Table 1) are characteristic of stoichiometric magnetite [25]. The slightly wider Verwey transition seen in Fig 2a, suggests that some of the grains in the *W(11 μm)* assemblage may have undergone partial surface oxidation. That *E(2 mm)* does not demagnetize to the same extent as *H(23 μm)* on warming through the Verwey transition is partially due to the visible impurities in the sample.

The viscosity measurements were made using a Quantum Design magnetic properties measurement system (MPMS). Both acquisition and decay of viscous magnetization were measured; acquisition in a field of 0.5 mT, and decay in the "zero-field" state of the MPMS (± 0.5 μT). The samples were dispersed by about 5% concentration in silicone grease. Initially the samples were alternating field (AF) demagnetized in three directions using a maximum field of 100 mT. Before the initial viscous measurement and between each subsequent viscous measurement, the samples were cycled through T_V. Such low-temperature cycling is known to demagnetize soft remanences [24]. The reason for doing this rather than AF demagnetize the samples between each was to make use of the automated sequence procedure available on the MPMS. Finally, to minimize the time between measurements, the data was collected with no averaging, which is normally standard for the MPMS. This was particularly important for the initial points of each measurement, due to the logarithmic nature of viscous behavior. The first data point was collected approximately 20 s seconds after switching on/off the field.

3 Experiments

3.1 Viscous magnetization versus temperature

Typical acquisition and decay curves are shown for *W(11 μm)* (Fig. 3). The acquisition and decay of magnetization *M* vary with time *t* as a first approximation by $M \propto \log(t)$. The gradient of this slope ($\partial M / \partial \log(t)$) is commonly referred to as the viscosity coefficient *S*, where S_A and S_D represent the acquisition and decay coefficients respectively. S_A and S_D are plotted as a function of temperature for all three samples in Fig. 4. Before fitting S_A and S_D to the data as in Fig. 3, some data reduction was carried out to reduce biasing, in that the data was collected linearly in time. The subsequent data files were averaged over equal increments of log(*t*), i.e., $\log(t_{i+1})-\log(t_i)=0.1$, where *t* is time, and *i* the measurement step. The octahedral single crystal *E(2 mm)* was orientated on a surface, such that the field was applied along a <111> direction. This orientation was chosen since direct observations of viscous behavior above room temperature found that grains orientated on the {111} surfaces displayed greater viscosity compared to other orientations [26].

Generally the viscous behaviour for all three samples is observed to be similar (Fig. 4). With increasing temperature, samples *W(11 μm)* and *E(2 mm)* display a narrow peak at 10-20 K. Between ~50 K and T_V, all three samples display a broad plateau. For samples *W(11 μm)* and *H(23 μm)* this plateau contains two distinct peaks; one at ~70-90 K and the other just below T_V. *E(2 mm)* displays only one peak just below T_V. Above T_V, in all three samples S_A and S_D are greatly reduced, but increase gradually on warming to 300 K. Samples *W(11 μm)* and *H(23 μm)* display a broad peak centered at 160-200 K. The large drop in viscosity rate on warming through T_V is greater than that reported in other studies for SD [5] and MD [22] magnetite.

The ratio S_A/S_D allows for the comparison of acquisition and decay mechanisms. Most MD thermal fluctuation theories predict S_A/S_D = 1 [8, 27, 28]. In contrast, Néel's [6] thermal fluctuation model predicts S_A/S_D = 2. In this study, it is seen that generally S_A is greater than S_D (Fig. 5), except for *E(2mm)* for temperatures above T_V where both S_A and S_D were both very small (Fig. 4c). For all three samples, below T_V the ratio S_A/S_D varies between 1 and 2, but above the transition the variation is much greater. Both *W(11 μm)* and *H(23 μm)* display a distinctive broad peak in S_A/S_D centred on 160 K. This is probably related to the peaks observed in both S_A and S_D between 160-200 K (Figs. 4a and 4b).

3.2 Non-log(t) behavior

It was assumed in section 3.1 that the viscosity varies linearly as log(*t*), however, this is only a first-order approximation and non-linear behavior is commonly observed in both SD and MD assemblages. In Fig. 6 three acquisition curves are shown for *W(11 μm).* The 10 K and 40 K curves display slight upward curvature and the 20 K curve slight downward curvature. Due to our lack of understanding of MD viscous theory, it is difficult to attribute this non-linearity to a specific mechanism, however, viscous SD theory predicts such non-log(*t*) behavior if magnetostatic interactions and/or grain distributions are included . To access this non-log(*t)* behavior it has been common to assume a second-order polynomial of the form

$$M = \alpha + \beta \log(t) + \gamma \log(t)^2 \qquad (1)$$

where α, β and γ are fitted coefficients. For acquisition data where the slopes are positive, an acceleration in the slope is indicated by a positive curvature parameter γ_A (the 10 K and 40 K curves in Fig. 6). Similarly, for viscous decay the slope is negative, therefore an increase in the slope is indicated by γ_D being negative.

In Fig. 7, γ_A and γ_D are plotted as a function of temperature for samples *W(11 μm), H(23 μm)* and *E(2 mm)*. Generally, with a couple of notable exceptions and for $T > T_V$ for *E(2mm),* γ_A is

positive and γ_D is negative. The exceptions occur < 40 K in all three samples. The overall behavior is in many respects similar to that observed for of the S_A and S_D (Fig. 4), i.e., γ_A and γ_D are relatively larger below T_V than above it, and *W(11 μm)* and *H(23 μm)* display increased curvature between 160 K and 200 K. Interestingly γ_A and γ_D mirror each other regardless of their sign. For example, γ_A and γ_D both switch signs for one measurement point in *W(11 μm)* at 20 K (Figs. 6 and 7a).

4 Discussion

On comparison with the work of Walz and others [11, 15, 18, 29], it is apparent that below room temperature the viscosity of MD magnetite is strongly related to the disaccommodation spectra (Figs. 1 and 4). This correlation is unsurprising, as both spectra are determined from time-dependent weak-field magnetic measurements. However, the temperatures of the peaks and troughs are a little lower in the viscosity spectra than in most of the disaccommodation spectra. There are two possible causes for these differences. First, the different timescales of the measurements are likely to be important as the positions of the peaks in the disaccommodation spectra are known to be time dependent; the peaks shift to lower temperatures as the measurement time increases due to the thermally activated nature of the processes contributing to disaccommodation. For example, for a polycrystalline magnetite sample a disaccommodation peak located at ~320 K measured at 2 s, shifted to ~290 K on measuring after 180 s [30]. As the viscosity measurements were made over longer timescales, i.e., > 2000 s, it would be expected that the positions of the viscosity peaks would be shifted to even lower temperatures. More importantly, however, the viscosity parameter S_A is in effect the rate of change of disaccommodation spectra with time at a given temperature; if disaccommodation peaks are decreasing in temperature with time, then S_A will be greatest at lower temperatures. Second, there is also considerable variation in the disaccommodation spectra peak temperatures for magnetites from different origins [11, 30].

Assuming this correlation disaccommodation and viscosity, then the various physical mechanisms thought to control disaccommodation can also be attributed to the observed

viscosity. “Perfect magnetite” has a long-range electron tunneling plateau with an adjoint Debye peak [31] in the region 4 K to T 25 K (Fig. 1) [11]. Electron hopping processes give rise to another plateau in the range 50 K to T_V. Any kind of lattice perturbation such as thermally induced vacancies, internal stresses, intrinsic defects, ion substitution etc. will affect or destroy these order-dependent electronic relaxations [29, 32]. Above T_V there is weak disaccommodation process attributed to polaron conduction [33] with a small stoichiometry dependence (Fe_3O_{4+x}, $0.002 \leq x \leq 0.035$) within the range $T_V \leq T \leq 250$ K [34, 35]. A little above the temperatures reported in this paper, there is a significant Debye process at ~300 K, which is induced by B-site vacancies.

Samples *W(11 μm)* and *E(2 mm)* both displayed a large peak in S_A in the temperature range 4 K to T 25 K, though at 20 K the position of the peaks were a little lower than the Debye peak at ~30 K. *H(23 μm)* displayed a relatively smaller peak in S_A at 20 K. Within this low-temperature electron tunneling plateau the curvature parameters γ_A and γ_D both showed erratic behavior, switching signs between 10-40 K (Figs. 6 and 7). It appears that where disaccommodation is at its greatest (Fig. 1), γ_A and γ_D reverse sign making γ_A negative and γ_D positive. S_A and S_D display high values in the range 50 K to T_V, i.e., the electron hopping plateau. *W(11 μm)* and *H(23 μm)* display two peaks, however, this does not appear to correlate directly with the disaccommodation spectra, which typically display only one peak at 60-70 K in the hopping plateau. This double peak is also observed in γ_A and γ_D for *H(23 μm)*. Above the T_V, both *W(11 μm)* and *H(23 μm)* display small peaks in S_A, S_D and γ_A and a trough in γ_D in the range 160 K -200 K. This is probably associated with polaron conduction, and may reflect very low-levels of non-stoichiometry in the samples. In this temperature range γ_A and γ_D display a change in sign and a peak for sample *E(2 mm)*.

If disaccommodation has the effect of reducing S_A and S_D with time as predicted by Moskowitz [1], then disaccommodation should cause γ_A to be negative and γ_D positive. For *W(11 μm)* and *H(23 μm)* it is only at the peak in S_A and S_D in the range ~10 - 20 K, that γ_A is negative and γ_D positive, suggesting that disaccommodation is not contributing significantly to

the observed viscous effect. However, the strong correlation between S_A and S_D and disaccommodation spectra (Figs. 1 and 4), both experimentally and from a theoretical point of view, suggest the opposite. For example, the electron hopping plateau in the range 50 K to T_V, is readily identifiable in the viscosity data (Fig. 4). Thus the curvature observed in the viscous data must have another origin. Dislocation creep which is known to cause curvature [10], can be ruled out due to the thermal history of the samples. This leaves the probability that the shape of the curvature is controlled by relaxation-time distributions - effectively coercive force distributions - within the grains. Tropin [36] demonstrated that by expedient choice of distribution function any type of viscosity behavior can be obtained. The fact that at any temperature for samples from different origins, the curvature parameters γ_A and γ_D are usually positive and negative respectively [10], suggests the shapes of relaxation-time distributions within MD magnetite assemblages have common key features.

Some of the differences in behavior observed between the W*(11 μm)* and *H(23 μm)* samples and *E(2 mm),* are probably due to the latter being a single orientated crystal compared to an assemblage, i.e., the observed behavior might be particular to that orientation. Assuming a single overall domain orientation in the grain, above T_V the domain orientation could take one of four directions, making possible interpretations of the data difficult. Below T_V the monoclinic structure can take one of several possible orientations with respect to the {111} surface, giving rise again to multiple interpretations. In addition it is very likely that in such a large grain in the monoclinic phase crystallographic twins will form [37], adding to the difficulty in interpreting the data.

The curvature parameters γ_A and γ_D with one or two exceptions consistently mirror each other throughout the entire temperature range (Fig. 7). This suggests that the acquisition and decay processes are identical, with S_A being greater than S_D due to the statistical nature of viscous acquisition and decay. Simple statistics tells us that if a sub-set of grains from an assemblage acquires a magnetization by stochastic processes in time t_a, then even if the relaxation process in zero-field is identical, the amount of time for this smaller sub-set of particles to relax and completely demagnetize will be statistically greater than t_a.

5. Conclusions

On measuring the low-temperature viscosity spectra of MD magnetite a strong correlation with the disaccommodation spectra has been found. It is proposed that the reduction in electron mobility which gives rise to the disaccommodation spectra controls the large increase observed in the viscosity below T_V. Between T_V and 275 K, the increase in electron mobility results in both a reduction in disaccommodation and viscosity as found in this study.

It appears that disaccommodation and viscosity are closely related, however, between T_V and the Curie temperature generally disaccommodation processes in magnetite are quite low with the exception of the significant Debye peak at ~300 K, which is strongly dependent on B-site vacancies, i.e., non-stoichiometry. Attempts to assess the importance of disaccommodation processes on the magnetic viscosity using experiments conducted solely at room temperature [1, 38], may have over-estimated disaccommodation's overall contribution to the viscosity.

On comparison with the low-temperature SD data of Worm et al. [5], it would appear that disaccommodation processes can also affect the viscosity of SD grains.

Disaccommodation processes do not appear to control γ_A and γ_D. It is suggested that they are controlled by the shape of relaxation-time distributions, which have approximately the same general features independent of the magnetite's origin. In addition, γ_A and γ_D mirror each other when plotted as a function of temperature, inferring that at any given temperature the acquisition and decay processes are identical.

Acknowledgments

This work was funded through NERC research grant NER/A/S/2001/00539 to W.W. with additional funding from the Royal Society. Special thanks go to the Chinese Academy of Sciences, in particular Profs. Pan and Zhu, who were supportive and sponsored the MPMS

measurements in Beijing. We would like to thank Dr. Nic Odling for his help with the hydrothermal re-crystallization technique.

References

[1] B.M. Moskowitz, Geophys. J. R. astr. Soc. 82 (1985) 143–161.
[2] D. Walton, Nature 286 (1980) 245-247.
[3] L. Néel, Ann. Géophys. 5 (1949) 99–136.
[4] D. Walton, Nature 305 (1983) 616-619.
[5] H.-U. Worm, M.J. Jackson, S.K. Banerjee, C.M. Schlinger, J. Appl. Phys. 70 (1991) 5533–5537.
[6] L. Néel, J. Phys. Rad. 11 (1950) 49–61.
[7] V.S. Aver'yanov, Izv., Phys. Solid Earth 8 (1967) 531-536.
[8] F.D. Stacey, Adv. Phys. 12 (1963) 45–133.
[9] Y.D. Tropin, I.M. Belous, I.A. Stretskul, Izv., Phys. Solid Earth 1 (1973) 61-62.
[10] W. Williams, A.R. Muxworthy, J. Geophys. Res. 111 (2006) doi:10.1029/2005JB003695.
[11] F. Walz, J. Phys.-Cond. Matter 14 (2002) R285-R340.
[12] L. Néel, J. Physique 13 (1952) 249–254.
[13] L.Y. Sholpo, Izv., Phys. Solid Earth 6 (1967) 390-399.
[14] S.L. Halgedahl, J. Geophys. Res. 98 (1993) 22,443–422,460.
[15] F. Walz, H. Reule, M. Hirscher, H. Kronmüller, Phys. Stat. Sol. (B) 241 (2004) 389-400.
[16] V.I. Trukhin, Izv., Phys. Solid Earth 4 (1972) 235-241.
[17] J. Garcia, G. Subias, J. Phys.-Cond. Matter 16 (2004) R145-R178.
[18] F. Walz, L. Torres, C. Defrancisco, J. Iniguez, H. Kronmüller, Phys. Stat. Sol. (A) 163 (1997) 233-246.
[19] K. Abe, Y. Miyamoto, S. Chikazumi, J. Phys. Soc. Japan 41 (1976) 1894-1902.
[20] L.R. Bickford, J.M. Brownlow, R.F. Penoyer, Proc. I.E.E.E. B104 (1957) 238-244.
[21] A.R. Muxworthy, E. McClelland, Geophys. J. Int. 140 (2000) 101-114.
[22] Y. Shimizu, J. Geomag. Geoelec. 11 (1960) 125–138.
[23] F. Heider, L.T. Bryndzia, J. Crys. Growth 84 (1987) 50–56.
[24] A.R. Muxworthy, E. McClelland, Geophys. J. Int. 140 (2000) 115-131.
[25] Ö. Özdemir, D.J. Dunlop, B.M. Moskowitz, Geophys. Res. Lett. 20 (1993) 1671–1674.
[26] A.R. Muxworthy, W. Williams, J. Geophys. Res. B (2006) doi:10.1029/2005JB003902.
[27] G. Richter, Ann. Physik 29 (1937) 605–635.
[28] R. Street, J.C. Woolley, Proc. Phys. Soc. London (A) 62 (1949) 562–572.
[29] L. Torres, F. Walz, C. Defrancisco, J. Iniguez, Phys. Stat. Sol. (A) 163 (1997) 221-231.
[30] F. Walz, L. Torres, K. Bendimya, C. de Francisco, H. Kronmüller, Phys. Stat. Sol. (A) 164 (1997) 805-820.
[31] A.H. Morrish, Kreiger, Florida, 1965, 680 pp.
[32] H. Kronmüller, F. Walz, Phil. Mag. B 42 (1980) 433-452.
[33] C. Kittel, Wiley & Sons, New York, 1975, 608 pp.
[34] S. Todo, K. Siratori, S. Kimura, J. Phys. Soc. Japan 64 (1995) 2118-2126.
[35] S. Nakamura, L. Li, M. Tanaka, S. Todo, K. Siratori, J. Phys. Soc. Japan 66 (1997) 472-477.
[36] Y.D. Tropin, Izv., Phys. Solid Earth 7 (1970) 454-456.
[37] C. Medrano, M. Schlenker, J. Baruchel, J. Espeso, Y. Miyamoto, Phys. Rev. B 59 (1999) 1185-1195.
[38] M.A. Tivey, H.P. Johnson, J. Geophys. Res. 89 (1984) 543–552.

Tables

Table 1. Physical, chemical and magnetic properties of the nine samples.

Sample name	Grain size (μm)	$\mu_0 H_C$ (mT)	$\mu_0 H_{CR}$ (mT)	H_{CR}/H_C	M_{RS}/M_S	Verwey temp. (K)	Chemical description
W(11 μm)	11 (3)[a]	4.5	17	3.8	0.07	122	magnetite
H(23 μm)	23(5)	0.9	21	23	0.006	125	magnetite
E(2 mm)	2000	0.3[b]	8.9[b]	30[b]	0.002[b]	117	magnetite + trace of hematite

The grain-size distributions for samples were determined from scanning electron micrographs, except for sample *E(2 mm).* The grain-size standard deviations are shown in brackets. The chemical composition was determined from Mössbauer, XRD and magnetic analysis .

[a] mean aspect ratio =1.8.

[b] field applied in a <111> direction.

Figure Captions

Figure 1. Low-temperature disaccommodation (or MAE) spectrum for a single crystal of stoichiometric magnetite between 4 K and 125 K. Above 125 K, i.e., the Verwey transition, the disaccommodation is greatly reduced. The disaccommodation spectrum is defined as $\Delta r/r1(\%) = [r(t_2) - r(t_1)]/r(t_1)$, where $r(t)$ is the reluctivity and is defined as $r = 1/\chi$, where χ is the susceptibility and t time [11]. The measurements were made between 2 s and 180 s after demagnetization. The initial susceptibility χ_0 (arbitrary units) is also shown. Redrawn with permission from Walz et al. [15].

Figure 2. Warming curves for SIRM induced at 5 K in a field of 2 T, for the three samples in the study. The first derivative dM/dT is also shown to help identify the Verwey temperature (Table 1). For ideal magnetite the Verwey transition is 125 K.

Figure 3. Acquisition and decay of viscous magnetization for sample *W(11 μm)* at 120 K plotted on a logarithmic time scale with simple linear regression fit. Acquisition field was 0.5 mT.

Figure 4. Viscosity acquisition and decay coefficients S_A and S_D versus temperature for (a) *W(11 μm)*, (b) *H(23 μm)* and (c) *E(2 mm)*. Acquisition field was 0.5 mT. The octahedral single crystal *E(2 mm)* was orientated on a surface, i.e., the field was applied approximately in the <111> direction. The y-axis error bar is determined from the error in the least-squares fit of S_A and S_D. There was very little error in the x-axis, due to the high accuracy of temperature control in the MPMS.

Figure 5. Ratio S_A/S_D versus temperature for *W(11 μm)*, *H(23 μm)* and *E(2 mm)*.

Figure 6. Viscous acquisition curves for *W(11 μm)* at 10 K, 20 K and 40 K. The 10 K and 40 K acquisition curve show positive curvature whilst the 20 K acquisition curve, negative curvature. The applied field was 0.5 mT.

Figure 7. Curvature parameters γ_A and γ_D versus temperature for (a) *W(11 μm)*, (b) *H(23 μm)* and (c) *E(2 mm)*. Acquisition field was 0.5 mT.

Figures

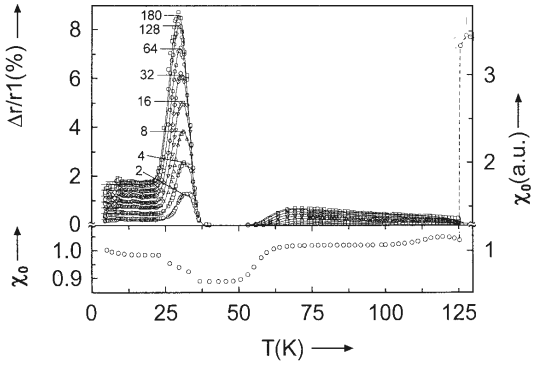

Figure 1

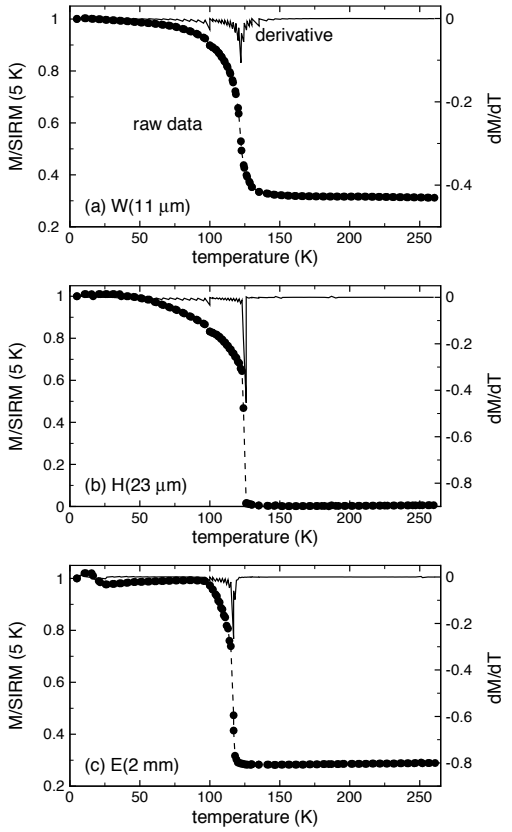
derivative
raw data
(a) W(11 μm)
(b) H(23 μm)
(c) E(2 mm)
M/SIRM (5 K)
dM/dT
temperature (K)

Figure 2

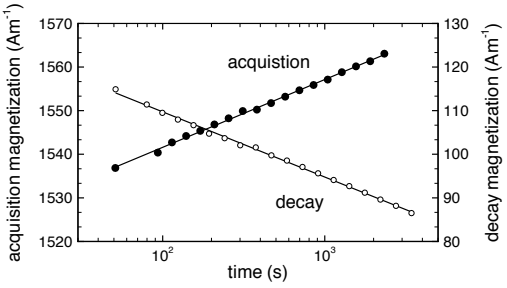
acquisition magnetization (Am-1)
decay magnetization (Am-1)
1570
1560
1550
1540
1530
1520
130
120
110
100
90
80
acquistion
decay
10^2
10^3
time (s)

Figure 3.

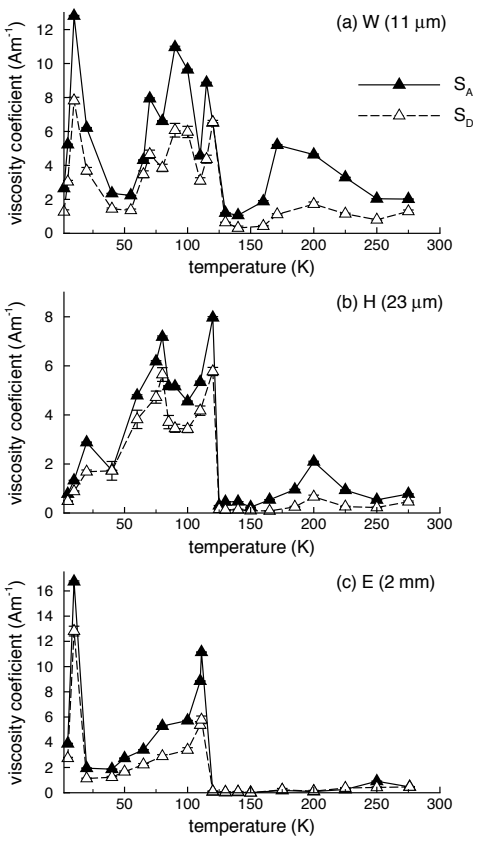
(a) W (11 μm)
S_A
S_D
viscosity coeficient (Am^{-1})
temperature (K)
(b) H (23 μm)
viscosity coeficient (Am^{-1})
temperature (K)
(c) E (2 mm)
viscosity coeficient (Am^{-1})
temperature (K)

Figure 4.

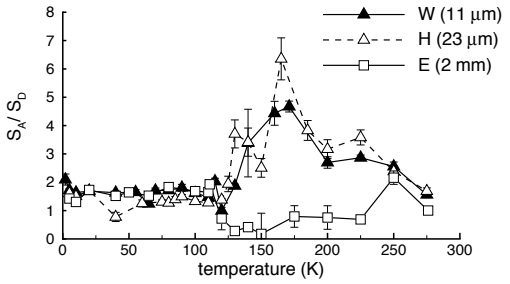
W (11 μm)
H (23 μm)
E (2 mm)
S_A / S_D
temperature (K)
0
1
2
3
4
5
6
7
8
0
50
100
150
200
250
300

Figure 5.

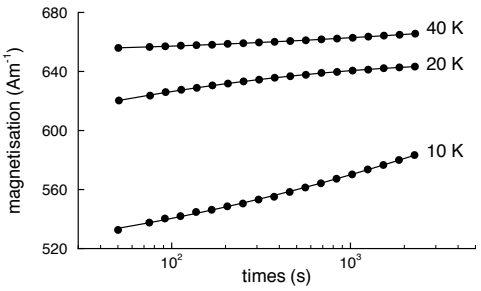
680
640
600
560
520
magnetisation (Am-1)
40 K
20 K
10 K
10^2
10^3
times (s)

Figure 6.

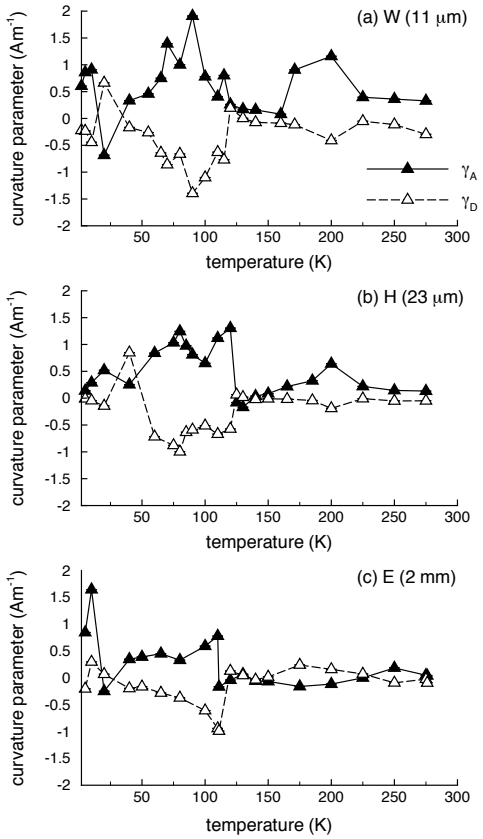
(a) W (11 μm)
(b) H (23 μm)
(c) E (2 mm)
curvature parameter (Am-1)
temperature (K)
γA
γD

Figure 7.